J. Fluid Mech. (1991), *vol.* 232, *pp.* 341–355
Printed in Great Britain

Analysis of swimming three-dimensional waving plates

By JIAN-YU CHENG, LI-XIAN ZHUANG AND BING-GANG TONG

Department of Modern Mechanics, University of Science and Technology of China, Hefei, Anhui, China

(Received 7 December 1989 and in revised form 15 January 1991)

The three-dimensional waving plate theory is developed to investigate the swimming performance of fish undulatory motion. In particular, the propulsive effectiveness is discussed. The unsteady potential flow over model rectangular and triangular flexible plates performing a motion which consists of a progressing wave with variable amplitudes is calculated by the vortex ring panel method. It is found that the undulatory motion can reduce three-dimensional effects. It is this important hydrodynamic phenomenon that may be one of the main reasons why such undulation is widely used as the swimming method by a large number of aquatic animals. When the span of the undulating plate is nearly unchanged and the wave amplitude is constant or increases slightly along the chord, and the wavelength is close to the body length, theoretical results show that the swimming performance is best and the flow around the plate has a quasi-two-dimensional property. This swimming method may be observed in many fishes, especially those with an anguilliform mode of propulsion. The modification of the anguilliform mode of propulsion to the carangiform mode is also discussed. It is confirmed that the pronounced necking of the body anterior to the tail, which acts to improve the propulsive performance, is a major morphological adaptation of fishes using the carangiform mode, in which the characteristic nature of flexural movement confined to the rear part of the body is that the amplitude of undulation increases posteriorly and no complete wavelength is at any time apparent.

1. Introduction

The undulation propulsion method, in which a transverse wave passes backwards along the body from head to tail, is widely employed by a large number of aquatic animals, such as fishes and some cetaceans. This propulsive means, together with its various modifications, has been successful for aquatic animals' locomotion in a wide range of Reynolds numbers, R, based on the animal's length and forward velocity. The movements of most fishes correspond to the flow of large Reynolds numbers. Furthermore, characteristic propulsive modes in the great majority of fishes are broadly divided into two classes: anguilliform and carangiform. Fishes using the anguilliform mode are flexible over the whole body, and the propulsive wave travelling from head to tail has an amplitude which, although increasing posteriorly, is significant all along the fish's length. Carangiform propulsion may be considered as a development of the anguilliform mode. In this mode of swimming, the amplitude of undulation becomes significant only in the posterior half, or even one-third, of the fish; the remainder of the fish's body is relatively inflexible. In particular, the fastest

marine animals have adopted essentially the carangiform mode of propulsion, their tails having converged to a crescent-moon shape. This mode of swimming may be termed 'lunate-tail swimming propulsion'.

For 'elongated' fishes which are geometrically characterized by slender cylindrical forms, Lighthill (1975) developed the elongated-body reactive-force theory. Wu (1971) made further investigations on this problem. To analyse the swimming propulsion of the lunate tail, Lighthill (1975), Chopra (1974), Chopra & Kambe (1977), Lan (1979), Cheng & Murillo (1984) and Ahmadi & Widnall (1986) have used two- and three-dimensional unsteady wing theory to treat the problem like the flow past pitching and heaving rigid plates. Propulsion by median and paired fins is discussed by Blake (1983*a*, *b*). Recently, Karpouzian, Spedding & Cheng (1990) used their previously developed perturbation theory to analyse the performance of lunate-tail swimming propulsion. For both the anguilliform and carangiform modes of propulsion, however, the characteristic wavelike feature of the undulatory motion of the flexural body can be observed. Wu (1961) has given a theory on the motion of a two-dimensional waving plate.

Our purpose is to analyse the swimming propulsion of a more realistic model, i.e. a three-dimensional waving plate with variable amplitudes. Then, using this unified model we shall discuss the general hydrodynamic property of undulatory motion, and make a comparative systematic study on three classes of fish propulsion. An unsteady vortex ring panel method in the frequency domain, which can be applied to the undulatory motion of a flexible plate of general planform with small amplitude, has been developed by the present authors to analyse the swimming performance of a rectangular waving plate with constant amplitude (Cheng, Zhuang & Tong 1989). In this paper, the swimming performance of various rectangular and triangular waving plates with variable amplitudes is calculated to further analyse the three-dimensional effect and the swimming property of the anguilliform mode. The change from anguilliform motion to carangiform motion is also discussed. The application of optimum motion analysis to carangiform caudal-fin and lunate-tail propulsion will be given in papers.

Because the nonlinear features of the leading- and/or trailing-edge separation vortex are not very marked for cruising swimming of some fish, the present linear model and leading-edge suction treatment may be suitable for an elementary analysis. As has been done in modern computational aerodynamics (Kandil, Chu & Tureand 1982), the present method may be developed to consider the nonlinear and non-planar aspects of the vortical sheets separated from edges, which may influence performance characteristics. In fact, a nonlinear analysis of the two-dimensional incompressible flow around a flexible plate waving near a rigid wall has been given by Zhuang, Shida & Takami (1990). The extension to three-dimensional flow will be an important area of future study for considering the nonlinear effect of separated vortical sheets on swimming performance.

2. Formulation and energetics for a waving plate

It is assumed that a flexible thin plate of finite aspect ratio with a rounded leading edge and a sharp trailing edge is performing undulatory motion with small amplitude in a stream of incompressible invisid fluid of constant velocity U in the x-direction (figure 1). The wing planform is assumed to be symmetrical with respect to the x-axis and its shape is given by the leading-edge curve $x_{\mathrm{L}}(y)$ and trailing-edge curve $x_{\mathrm{T}}(y)$,

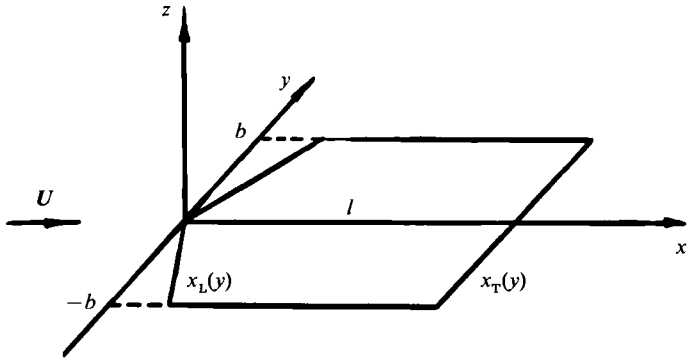

FIGURE 1. Definition sketch.

both of which are even functions of y. The lateral displacement in the z-direction is taken as a progressive planar wave of variable amplitude:

$$\begin{aligned} z &= \mathrm{Re}\,[h] \\ &= \mathrm{Re}\,[\tilde{h}(x,y)\,\mathrm{e}^{\mathrm{i}\omega t}] \\ &= \mathrm{Re}\,[H(x,y)\,\mathrm{e}^{\mathrm{i}(\omega t-kx)}], \end{aligned} \tag{1}$$

where Re stands for 'the real part of', $\omega = \sigma l/U$ is the reduced frequency referred to the length of the root chord l (σ being the circular frequency), and $k = 2\pi l/\lambda$ is the wavenumber (λ being the wavelength). U, l and l/U are taken as the reference velocity, length and time to normalize all physical parameters.

The wave amplitude $H(x,y)$ is taken as an arbitrary function of x as represented by a polynome, then

$$\begin{aligned} h(x,y,t) &= \sum_{n=1}^{M} a_n\, x^{n-1} \exp\,[\mathrm{i}(\omega t - kx)] \\ &= \sum_{n=1}^{M} A_n\, x^{n-1} \exp\,[\mathrm{i}(\omega t - kx + \psi_n)], \end{aligned} \tag{2}$$

where $a_n = A_n \exp\,(\mathrm{i}\psi_n)$ may be a complex function of y; however, at the present stage, we will not consider spanwise deformation so that a_n is chosen as a complex constant. Physically, the above expression and all the following complex quantities should be understood as their real parts.

The incompressible potential flow may be described by a velocity potential

$$\Phi(x,y,z,t) = x + \phi(x,y,z,t), \tag{3}$$

where Φ is the total potential and ϕ the perturbation potential, both of which satisfy Laplace's equation. The boundary condition on the wing surface that there is no penetration of the fluid across the solid boundary may be linearized as

$$\frac{\partial \phi}{\partial z} = \frac{\partial h}{\partial t} + \frac{\partial h}{\partial x} = \tilde{W}(x)\,\mathrm{e}^{\mathrm{i}\omega t}. \tag{4}$$

The expressions for the boundary conditions at the vortex wake surface and infinity as well as the Kutta condition at the trailing edge are given in the next section.

According to the unsteady Bernoulli's equation, the non-dimensional pressure difference across the plate is

$$\Delta C_p = C_{pl} - C_{pu} = 2\left(\frac{\partial \Delta\phi}{\partial t} + \frac{\partial \Delta\phi}{\partial x}\right) \tag{5}$$

where $\Delta\phi = \phi_u - \phi_l$, and the subscript u and l denote the values on the upper and lower surfaces respectively. To the linear approximation, we have

$$\left.\begin{aligned} \phi &= \tilde{\phi}(x,y,z)\,e^{i\omega t}, \\ \Delta\phi = \Delta\tilde{\phi}\,e^{i\omega t}, &\quad \Delta C_p = \Delta\tilde{C}_p\,e^{i\omega t}. \end{aligned}\right\} \tag{6}$$

The main interest here is to calculate the thrust and propulsive efficiency. During the undulatory motion, the plate does work at a rate E, and generates a thrust T, which is required to overcome the viscous drag exerted on the animal when swimming with velocity U. The total forward thrust has two sources: the horizontal component of the normal force acting on the wing surface, T_p; and the suction force, T_s, acting on the rounded leading edge owing to the low pressure associated with the fast flow around it, which can be calculated by the Blasius theorem.

The non-dimensional coefficients for the power required, thrust from the normal force and from the suction force, can be written as

$$\left.\begin{aligned} \hat{C}_E &= \frac{E}{qSU} = \frac{1}{S}\iint_{F_s} \mathrm{Re}\,[-\Delta C_p]\,\mathrm{Re}\left[\frac{\partial h}{\partial t}\right] dS \\ &= C_E + C_{E1}\cos 2\omega t + C_{E2}\sin 2\omega t, \\ \hat{C}_{T_p} &= \frac{T_p}{qS} = \frac{1}{S}\iint_{F_s} \mathrm{Re}\,[\Delta C_p]\,\mathrm{Re}\left[\frac{\partial h}{\partial x}\right] dS \\ &= C_{T_p} + C_{T_{p1}}\cos 2\omega t + C_{T_{p2}}\sin 2\omega t, \\ \hat{C}_{T_s} &= \frac{T_s}{qS} = \frac{2\pi}{S}\int_{-b}^{b} \mathrm{Re}\,[K_u]\,\mathrm{Re}\,[K_u]\,dy \\ &= C_{T_s} + C_{F_{s1}}\cos 2\omega t + C_{T_{s2}}\sin 2\omega t, \end{aligned}\right\} \tag{7}$$

where C_E, C_{T_p} and C_{T_s} are their time average values, which are given by

$$\left.\begin{aligned} C_E &= -\frac{1}{2s}\iint_{F_s} \mathrm{Re}\left[\Delta\tilde{C}_p \frac{\partial \tilde{h}^*}{\partial t}\right] dS, \\ C_{T_p} &= \frac{1}{2S}\iint_{F_s} \mathrm{Re}\left[\Delta\tilde{C}_p \frac{\partial \tilde{h}^*}{\partial x}\right] dS, \\ C_{T_s} &= \frac{\pi}{S}\int_{-b}^{b} \mathrm{Re}\,[\tilde{K}_u \cdot \tilde{K}_u^*]\,dy. \end{aligned}\right\} \tag{8}$$

In the above expressions,

$$K_u = \lim_{x \to x_L} u(x,y,t)\,(x - x_L)^{\frac{1}{2}},$$

* denotes the conjugate of a complex quantity, q is the dynamic pressure, and $u = (\partial\phi/\partial x)|_{z=0}$ is the x-component of perturbation velocity in complex form.

The thrust contribution from the leading-edge suction is represented by the ratio

$$\gamma_s = C_{T_s}/C_T = C_{T_s}/(C_{T_s}+C_{T_p}), \tag{9}$$

and we are interested in this since a very high leading-edge suction may lead to boundary-layer separation, which may cause a considerable thrust reduction. The hydromechanical propulsive efficiency of swimming is defined as

$$\eta = \bar{T}U/\bar{E} = C_T/C_E. \tag{10}$$

The importance of this parameter has been realized because of the impressive capability of some animals to generate fast movements at low energy cost.

The coefficient of side force L (lifting force) acting on the solid plate is

$$C_L = \frac{L}{qS} = \frac{1}{S}\iint_{F_s} \Delta C_p \, \mathrm{d}S = \tilde{C}_L \, \mathrm{e}^{\mathrm{i}\omega t}. \tag{11}$$

The coefficient of the yawing moment M (pitching moment) about the axis $x = a$, $z = 0$ is

$$C_M = \frac{M}{qSl} = -\frac{1}{Sl}\iint_{F_s} \Delta C_p(x-a) \, \mathrm{d}S = \tilde{C}_M \, \mathrm{e}^{\mathrm{i}\omega t}. \tag{12}$$

These side forces, fluctuating from side to side as the fish's body undulates, can cause an additional body movement which may be thought of as a sort of recoil process. Generally, large recoil movements should be avoided.

3. Unsteady vortex ring method applied to a waving plate

In potential flow theory, the vortex is restricted to an infinitely thin layer attached to the body surface which separates into a wake. It is this vortex sheet that results in the swimming propulsion. The basic idea of the vortex ring method is that the wing and its wake, both being in the $z = 0$ plane in the present linear theory, are replaced by a suitable distribution of vortex rings, which cause the boundary conditions of unsteady potential flow past a flexible plate to be satisfied.

Because of the symmetry with respect to the x-axis, the problem can be described in half-space. The planform is divided into small trapezoidal panels by Lan's 'semicircle' method (Lan 1979). A vortex ring is placed on each of the panels such that the vortex lines coincide with its perimeter. Let $N = N_s + N_w$ be the total number of vortex rings, N_s and N_w being the number of panels on the planform and wake respectively. The sequence number of panels may be specified as

$$\left.\begin{aligned} n &= p+(q-1)N_{sy} = (q,p), \\ p &= 1,\ldots,N_{sy}; \quad q = 1,\ldots,(N_{sx}+N_{wx}); \quad n = 1,\ldots,N, \end{aligned}\right\} \tag{13}$$

where N_{s_x} and N_{ws} are the numbers of chordwise panels on the planform and wake respectively, and N_{sy} is the number of spanwise panels.

The perturbation velocity V at any field point is equal to a finite sum of the induced velocities of all the vortex rings, i.e.

$$V = \sum_{n=1}^{N} \Gamma_n V_n \tag{14}$$

where Γ_n is the strength of each vortex rings, V_n the induced velocity due to a pair of vortex rings which are symmetric about the x-axis. The induced velocity of each

vortex segment of finite length may be calculated by the Biot–Savart law. Obviously, V thus obtained automatically satisfies the Laplace equation and the boundary condition at infinity that the perturbation velocity is approaching zero.

According to the Kelvin theorem, the rate of change of the circulation around a closed material curve is zero. Then, we get the boundary condition on the wake surface

$$\frac{\mathrm{d}\Gamma}{\mathrm{d}t} = 0. \tag{15}$$

The strength of vortex ring n on the wake, which can be obtained by (15), is

$$\left.\begin{aligned} \Gamma_n = \Gamma^{(q,p)} = \tilde{\Gamma}_{N_{Tp}} \exp\{-\mathrm{i}\omega[x_{cpq} - x_{\mathrm{T}}(y_{cp})]\} \exp(\mathrm{i}\omega t), \\ n = N_{\mathrm{s}}+1,\ldots,N; \quad p = 1,\ldots,N_{\mathrm{s}y}, \end{aligned}\right\} \tag{16}$$

where $N_{Tp} = p + (N_{\mathrm{s}x}-1)N_{\mathrm{s}y}$ $(p = 1,\ldots,N_{\mathrm{s}y})$, $\Gamma_{N_{Tp}}$ is the strength of rings next to the trailing edge. The Kutta condition at the trailing edge is given by

$$(\Delta C_p)|_{x=x_{\mathrm{T}}(y)} = 0. \tag{17}$$

From (5), we get the loading at panel n

$$\left.\begin{aligned} (\Delta C_p)_n = 2\Big\{\mathrm{i}\omega\tilde{\Gamma}_n + \frac{1}{2C_n}[(\tilde{\Gamma}^{(q,p)} - \tilde{\Gamma}^{(q-1,p)})\cos\chi^{(q,p)} \\ + (\tilde{\Gamma}^{(q+1,p)} - \tilde{\Gamma}^{(q,p)})\cos\chi^{(q+1,p)}]\Big\}\mathrm{e}^{\mathrm{i}\omega t}, \\ q = 1,\ldots,N_{\mathrm{s}x}; \quad p = 1,\ldots,N_{\mathrm{s}y}; \quad n = 1,\ldots,N_{\mathrm{s}}, \end{aligned}\right\} \tag{18}$$

where C_n is the mean chord length of the nth panel, $\chi^{(q,p)}$ the sweep angle of the vortex segment connecting the nodes (q,p) and $(q+1,p)$. It follows that (17) gives

$$\tilde{\Gamma}^{(N_{\mathrm{s}x},p)} = G\tilde{\Gamma}^{(N_{\mathrm{s}x}-1,p)}, \quad p = 1,\ldots,N_{\mathrm{s}y}, \tag{19}$$

where

$$G = \cos\chi^{(N_{\mathrm{s}x},p)}/[2\mathrm{i}\omega C^{(N_{\mathrm{s}x},p)} + (\cos\chi^{(N_{\mathrm{s}x},p)} - \cos\chi^{(N_{\mathrm{s}x}+1,p)}) + D^{(N_{\mathrm{s}x}+1,p)}\cos\chi^{(N_{\mathrm{s}x},p)}],$$

$$D^{(N_{\mathrm{s}x}+\nu,p)} = \exp\{-\mathrm{i}\omega[x_c{}^{(N_{\mathrm{s}x}+\nu,p)} - x_T(y_{cp})]\},$$

$$p = 1,\ldots,N_{\mathrm{s}y}; \quad \nu = 1,\ldots,N_{\mathrm{w}x}.$$

Substituting wake condition (16) and Kutta condition (19) into (14), we obtain

$$V = \tilde{V}\mathrm{e}^{\mathrm{i}\omega t} = \left(\sum_{n=1}^{N_{\mathrm{s}}-N_{\mathrm{s}y}} \Gamma_n K_n\right)\mathrm{e}^{\mathrm{i}\omega t}, \tag{20}$$

where

$$K_n = \begin{cases} V_n & (n \leqslant N_{\mathrm{s}}-2N_{\mathrm{s}y}) \\ V_n + G\left[V_{n+N_{\mathrm{s}y}} + \sum_{\nu=1}^{N_{\mathrm{w}x}} D^{(N_{\mathrm{s}x}+\nu,p)} V^{(N_{\mathrm{s}x}+\nu,p)}\right] & (N_{\mathrm{s}}-2N_{\mathrm{s}y} < n \leqslant N_{\mathrm{s}}-N_{\mathrm{s}y}). \end{cases}$$

The no-penetration condition, equation (4), is imposed at the control points. Thus, the resulting matrix equation of $(N_{\mathrm{s}}-N_{\mathrm{s}y})$ unknowns is written as

$$[\tilde{K}_{mn}]\{\tilde{\Gamma}_n\} = \{\tilde{W}_m\}, \tag{21}$$

where $\tilde{W}_m = \tilde{W}(x_{cm}, y_{cm})$ is determined by (4), $\tilde{K}_{mn} = (\tilde{K}_n \cdot n)_m$; $\tilde{K}_{mn}$, $\tilde{\Gamma}_n$ and $\tilde{W}_m$ are complex quantities. Equation (21) is solved to determine the $\tilde{\Gamma}_n$ which are then used to calculate the loading distribution and various energetics coefficients.

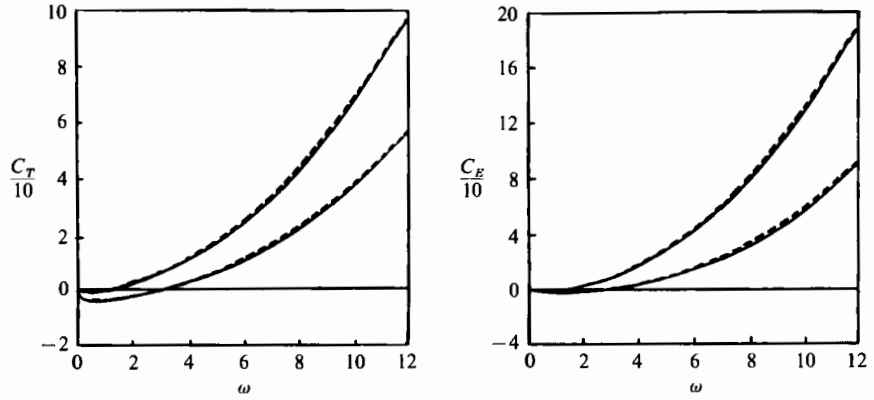

FIGURE 2. Comparison of thrust and power coefficients. Calculated by ——, present method; – – –, Wu's theory.

4. Analysis of swimming waving plates

The accuracy of the present method has been found to be reliable. For the rectangular waving plate with aspect ratio $A = 8$, figure 2 compares the variation of the thrust and power coefficients with reduced frequency from the present method with that from Wu's two-dimensional computations (Wu 1961), showing that reasonable results can be obtained by the present method. The swimming performance of several rectangular and triangular waving plates will be discussed in the following cases.

4.1. *Rectangular waving plate*

A variety of fishes have bodies, or at least their undulating parts, in a planar form of finite aspect ratio. The geometry of such fishes can reasonably be simplified as a rectangular thin plate whose undulatory motion with constant or increasing amplitude may represent some basic swimming characteristics of fishes, especially those with anguilliform mode.

In order to find the effect of the aspect ratio on the propulsive performance, we took (i) $A = 8$; (ii) $A = 1$; (iii) $A = 0.5$. The last two cases are close to those of many actual fish. Two important parameters of the undulatory motion are reduced frequency ω, with a value of around 10 based on the whole fish length for anguilliform motion (Lighthill 1975), and wavenumber k, giving the wave velocity $V_w = \omega/k$. It should be emphasized that the large value of the reduced frequency is suitable only for whole body undulation and cannot be used for modelling lunate tail propulsion for which ω is taken as around 1 based on tail length. The swimming of a waving plate of constant amplitude has been discussed in Cheng *et al.* (1989). Here, particular attention will be given to the effect of variable amplitude. The motion of a flexible plate is taken as

$$h = x^m \exp\,[\mathrm{i}(\omega t - kx)]. \tag{22}$$

Four undulation amplitude cases will be considered: values of the power of x in (22) of 0, 1, 2 and 3.

Figure 3 shows the thrust and efficiency against ω for the above four wave amplitudes at $k = 3$. Figure 4 shows the dependence of C_T and η on k at $\omega = 8$. From these figures, we can find:

(*a*) The forward thrust may be generated by the undulatory motion of a three-

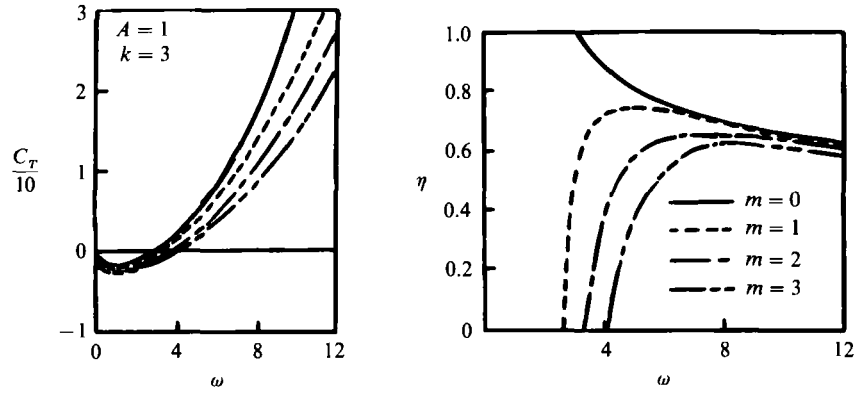

FIGURE 3. Thrust and efficiency variation with frequency for a rectangular waving plate with four kinds of amplitude variation.

dimensional flexible plate with constant or increasing amplitude. The propulsive efficiency is lower for waves progressing from tail to head (corresponding to $k < 0$) than those for waves progressing from head to tail (corresponding to $k > 0$), as indicated by Wu (1961) for two-dimensional waving plate analysis. This agrees with the observation that a large number of aquatic animals in nature move in the opposite direction to that of wave propagation at high Reynolds number, although it has been found that some polychaete worms move in the same direction (Lighthill 1975, pp. 15).

(*b*) Thrust may be produced only if the wave velocity ω/k is greater than a critical value, which is equal to the swimming velocity for a constant-amplitude wave and a little larger than the swimming velocity for an increasing-amplitude wave. This is also confirmed by observation.

(*c*) The thrust and power increase as the reduced frequency increases or the wavenumber decreases, while the values for the constant-amplitude wave are higher than the values for the increasing-amplitude wave.

(*d*) As the frequency increases, the propulsive efficiency increases rapidly from zero to its maximum value for the variable-amplitude case and decreases gradually from 1 for the constant-amplitude case. As the wavenumber increases, the efficiency increases linearly, but with a peak around $k = 6$ for the wave amplitude increasing markedly. Therefore, if the wave amplitude increases steeply, the wavenumber of undulation should be smaller than 2π, i.e. the wavelength of the progressing wave is larger than body length. It must be emphasized, of course, that this is for $\omega = 8$, when $k = 6$ corresponds to a wave velocity equal to $\frac{4}{3}$ of the swimming velocity.

(*e*) In general, the efficiency remains unchanged and the coefficients of thrust and power decrease as the aspect ratio decreases. When the wavelength is close to the body length, however, the thrust coefficient is nearly unchanged or even increases with decreasing aspect ratio. Consequently, in this case a reduction in size in the dorso-ventral direction of planar fishes results in no deterioration, and sometimes even an improvement, of propulsive performance.

The curves for lateral forces and moments against k at $\omega = 8$ for constant and linear amplitudes are plotted in figure 5. It can be seen that the absolute values of C_{LR}, C_{LI}, C_{MR} and C_{MI} for constant-amplitude waves are close to those for linear-amplitude waves, but their phases are different. The maximum values of these parameters are found in the diagram around $k = 0$, corresponding to the

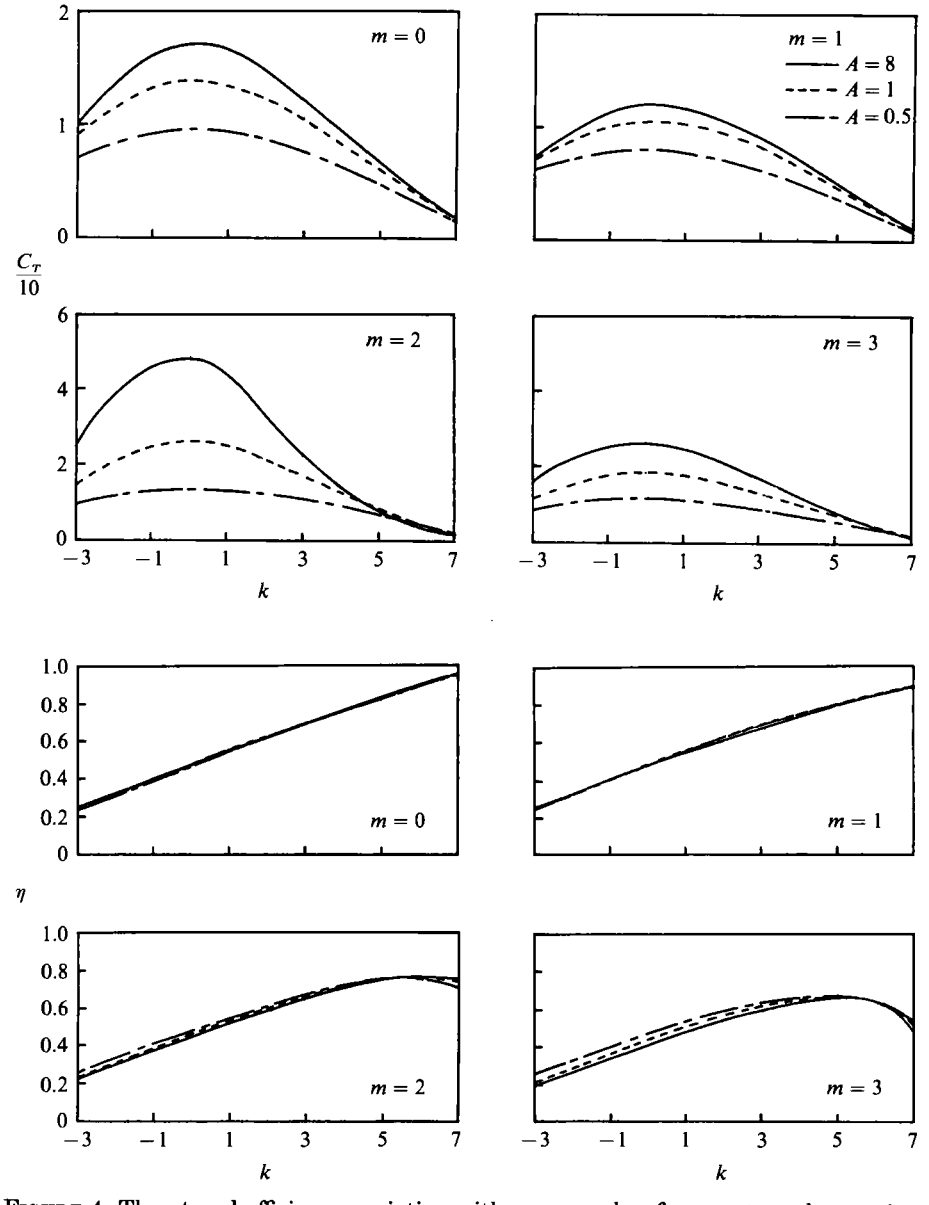

FIGURE 4. Thrust and efficiency variation with wavenumber for a rectangular waving plate with four kinds of amplitude variation and three values of aspect ratio.

pitching–heaving oscillation of a rigid plate. It is noted that for k larger than about 6, representing a progressing wave with about one wavelength along the body, all the in-phase and out-of-phase side forces and moments, especially for those of the constant-amplitude wave, vanish, producing the smallest recoil.

The variation of the ratio of the thrust due to leading-edge suction to the total thrust with k for constant- and linear-amplitude waves is shown in figure 6. For a constant-amplitude wave, the ratio decreases with increasing k for fixed ω or with decreasing ω for fixed k. For an increasing-amplitude wave, the ratio is very low

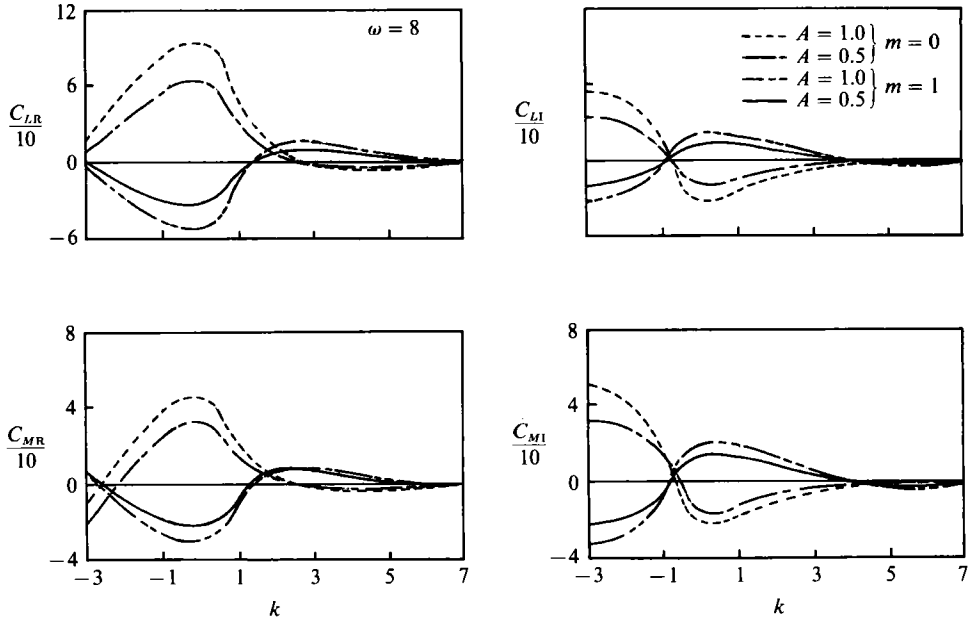

FIGURE 5. Side force and moment variation with wavenumber for a rectangular waving plate with two kinds of amplitude variation and two values of aspect ratio.

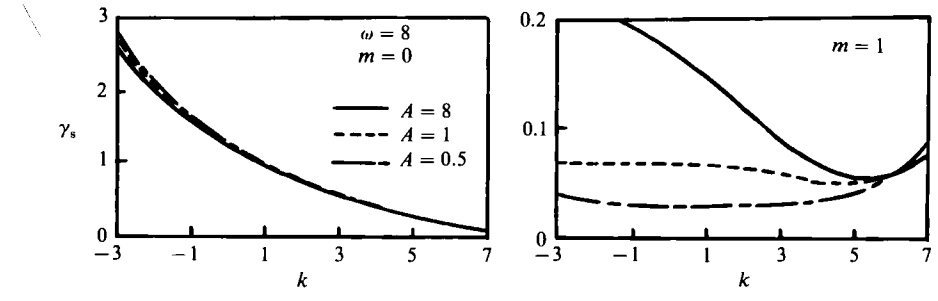

FIGURE 6. Leading-edge suction ratio variation with wavenumber for a rectangular waving plate with two kinds of amplitude variation and three values of aspect ratio.

because the undulation amplitude at the leading-edge becomes zero. Thus a larger wavenumber is advisable to avoid leading-edge separation.

4.2. *Discussion of the three-dimensional effect*

The three-dimensional effect of waving plates will be further discussed in this section. Computational results for small and large aspect ratio are compared with elongated body theory (Lighthill 1975) (denoted by EBT) and two-dimensional theory (Wu 1961) respectively.

According to Lighthill's theory, the propulsive efficiency is determined only by wave velocity V_W, i.e.

$$\eta = 1 - \frac{1}{2}\frac{V_W - 1}{V_W}. \tag{23}$$

Propulsive efficiency calculated by the present theory for a constant-amplitude wave with aspect ratio $A = 0.5$ is given in figure 7 in which two curves for η against

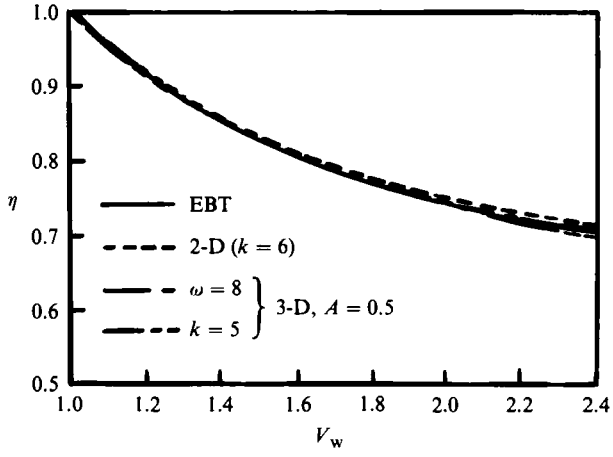

FIGURE 7. Comparison of efficiency calculated by present theory with that by other theories.

$V_W = 8/k$ and η against $V_W = \frac{1}{5}\omega$ are plotted. Wu's solution of a constant-amplitude waving plate at $k = 6$ and results of EBT are also drawn in the figure. It is found that all curves are close together. From the above section, it can be seen that efficiency is almost unaffected by aspect ratio. So the propulsive efficiency of three-dimensional waving plates with infinite to small aspect ratio is nearly the same as the results given by EBT, which are determined only by a combination of frequency and wavenumber, i.e. wave velocity $V_W = \omega/k$. It may be confirmed that this feature still exists for undulation amplitude increasing slowly along the body length. However, if the amplitude increases steeply, it follows from the previous discussion that the efficiency of the three-dimensional waving plate does not coincide with the result of EBT.

Let b_T denote the semispan of the trailing edge, the thrust coefficient obtained by EBT is

$$C_T = \tfrac{1}{2}\pi \frac{b_T^2}{S}(\omega^2 - k^2). \tag{24}$$

In figure 8, curves of C_T varying with ω at $k = 3$, obtained by the calculation of a three-dimensional waving plate with aspect ratios $A = 0.5$, 1.0 and 8, are compared with that by (24) letting $A = (2b_T)^2/S = 0.5$ and Wu's two-dimensional solution. In figure 9, curves for C_T varying with k at $\omega = 8$ are also shown. It can be seen that the three-dimensional solution for $A = 8$ is close to the two-dimensional solution, while the three-dimensional solution for $A = 0.5$ is close to the result of EBT. Consequently, for the swimming of an elongated flexible body, quite accurate results may be given by EBT for slenderness ratios up to 0.5. For larger aspect ratios, results of three-dimensional solutions show that in general EBT will not be valid. For higher values of k, however, figure 9 shows that thrust coefficient remains nearly unchanged with respect to aspect ratio; furthermore, C_T for large aspect ratio is even lower than that for small aspect ratio.

According to these comparisons, it may be confirmed that undulation of a flexible plate can reduce the effect of aspect ratio. When wavelength is close to body length, three-dimensional effects almost disappear, i.e. cross-sectional flow at any spanwise station for a rectangular flexible plate with arbitrary aspect ratio is approximately equivalent to two-dimensional flow, and the hydrodynamic properties of a small-

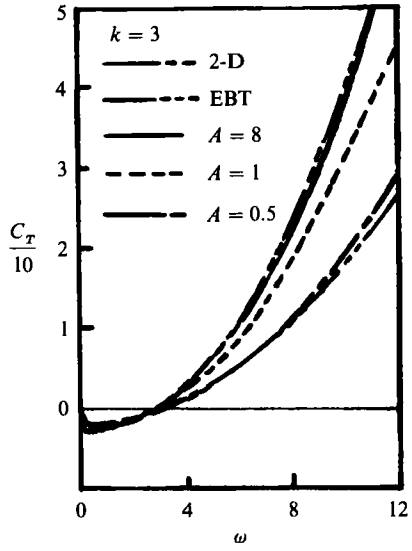

FIGURE 8. Comparison of thrust calculated by present theory with that by other theories.

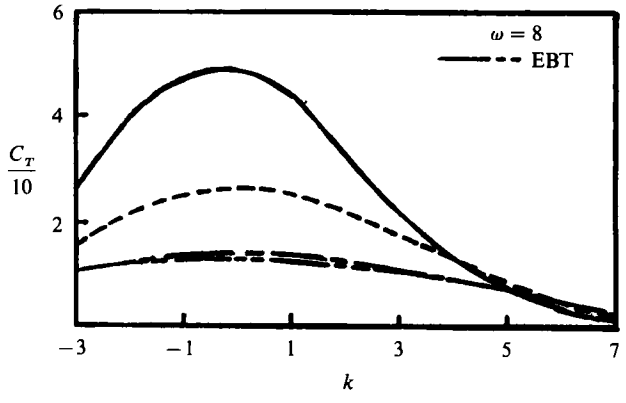

FIGURE 9. Comparison of thrust calculated by present theory with that by other theories.

aspect-ratio waving plate are close to those of an infinite-aspect-ratio waving plate. It can be imagined that in the flow pattern at the side edge of a waving plate, the flow tends to move from the lower surface to the upper surface along the chord segments from wave crest to wave trough, while it tends to move from the upper to the lower surface along the chord segments from wave trough to wave crest, so that the two streams of transverse flow partly cancel out and the spanwise flow is weakened. Furthermore, as pointed out by Cheng & Murillo (1984) (first noted by Cheng 1976), the self-averaging of the periodic wake structure may reduce three-dimensional effects for an oscillating wing when $\omega A \gg 1$. This is also true for the present case of a waving plate. So, the combination of the continuous waving deformation of the flexible plate and the self-averaging effect may result in considerable weakening of the chordwise vortex along the side edge and the spanwise flow on the plate surface and in the wake as the wavelength tends to body length. Thus, quasi-two-dimensional flow may exist for a waving plate of about one wavelength. Obviously, if the wave amplitude changes quickly along the body

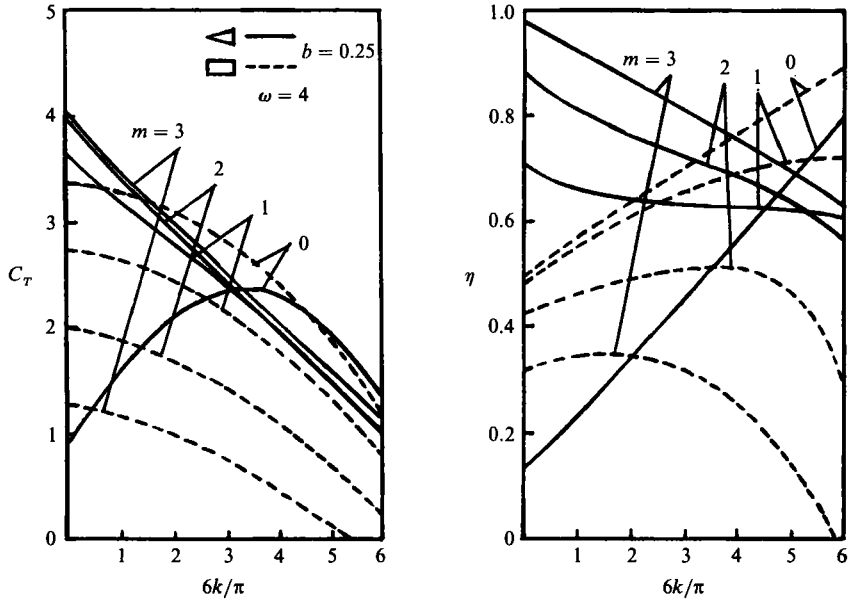

FIGURE 10. Thrust and efficiency variation with wavenumber for rectangular and triangular waving plates with four kinds of amplitude variation.

length, spanwise flow may be strengthened, and so the effect of aspect ratio is more marked.

4.3. *Modification of anguilliform to carangiform mode*

The carangiform mode of propulsion is found in a wide variety of fishes and sea animals. Lighthill (1975) proposed that fishes using the carangiform mode have certain important morphological characteristics in their posterior body, namely, necking of the body anterior to the caudal fin, and a deep cross-section near the mass centre to reduce recoil due to unbalanced oscillations of the side force. It is very important that the characteristic wavelike feature is retained within the region to which the undulations are confined in carangiform motion which is probably developed from the more obviously wavy anguilliform motion. In other respects, the wave amplitude (which increases gradually from head to tail in anguilliform motion) shows such a steep increase towards the tail in the last third of the body length that the observer of carangiform motion cannot see anything like a whole wavelength at any one time.

In the present study, propulsion achieved by the undulation of the posterior body modelled by a triangular waving plate will be considered. This model represents some features of the body shape for carangiform propulsion, i.e. the necking of the body anterior to the tail and the developed caudal fin. Observation shows that the reduced frequency based on the length of the undulating part of the body is about 4, and the wavenumber is 0 to π, owing to no complete wavelength being apparent.

The propulsive characteristics are calculated for a triangular plate and a rectangular plate, both with semispan $b = 0.25$ (the ratio of the semispan of trailing edge to the root chord), and with the four wave amplitudes shown in (22). The variation of these quantities with wavenumber at $\omega = 4$ is shown in figure 10. With the transition of anguilliform mode to carangiform mode, the confinement of undulations to a reduced fraction of the fish's length in the neighbourhood of the caudal fin is accompanied by the undulating amplitude increasing posteriorly from

a small value, or even zero, in the anterior region to a large value near the trailing edge, which corresponds to the variable-amplitude undulation of the last three cases in (22).

The curves of C_T show that with increasing k, thrust coefficients of the triangular plate, while decreasing and being close to each other for several variable-amplitude cases, are higher than those of the rectangular plate. The values of the efficiency of the triangular plate for amplitudes of the second and third power of x, and the first power of x at lower values of k, are also higher than those of the rectangular plate. This shows that for increasing wave amplitude the propulsive performance of the triangular plate is better than that of the rectangular plate, especially at lower wavenumbers. So when propulsion is mainly accomplished by the undulation of the posterior body and characterized by the carangiform mode, the pronounced necking of the body anterior to the tail and the developing of a caudal fin, forming a body shape similar to a triangular plate in lateral view, are important morphological adaptations of fishes and improve propulsive performance. However, the corresponding form of undulation is that no complete wavelength is at any time apparent, which may result in high propulsive efficiency.

For wave amplitude varying slowly along the body length, corresponding to a constant-amplitude wave, the efficiency of triangular plates is obviously lower than that of rectangular plates, and the thrust of triangular plates is lower than that of rectangular plates at lower values of k and both are close to each other at higher values of k. Therefore, for an undulation of nearly constant amplitude, the propulsive performance of a slender triangular plate is no longer better than that of a slender rectangular plate. This may explain the features of body shape and movement of fishes adopting anguilliform mode, i.e. body shape (depth in dorsal and anal direction) having no obvious variation along body length and wavenumber being higher.

5. Conclusion

Using the present linear three-dimensional waving plate theory, the swimming performances of undulatory motion of fish are discussed. The following conclusions may be drawn:

(i) Undulatory motion of a flexible plate may reduce three-dimensional effects, such as the effects of aspect ratio and the shape of the waving plate. It seems that a larger number of aquatic animals adopting undulation as their swimming means have utilized this hydrodynamic property.

(ii) Reasonable results may be obtained by the present three-dimensional waving plate theory for swimming propulsion of undulating plates with large and small aspect ratio. The present analysis shows that the elongated-body theory is valid over a wide range with respect ratio up to 0.5, as long as the undulation amplitude varies slowly along the body length and the chordwise variation of local span is small (being close to rectangular).

(iii) For the anguilliform mode of propulsion at a realistic reduced frequency, the swimming performance is best when the span of undulating plates is nearly unchanged and the wave amplitude is constant or increases slightly along body length, and approximately a complete wavelength is apparent at any time. Such features coincide with observation. Theoretical results also show that this mode has the properties of two-dimensional flow. Therefore, it is not difficult to understand that many fishes adopting the anguilliform mode have elongated planar form bodies.

(iv) In the modification of anguilliform to carangiform mode, the front half of the body loses its flexibility and flexural movement is confined to the rear half or even the rear third of the body. The propulsive performance of triangular plates is then notably better than that of rectangular plates, so the pronounced necking of the body anterior to the tail and the development of the caudal fin are important morphological adaptations and act to improve propulsive performance. At the same time the undulation whereby the wavelength is larger than the tail length (no complete wavelength is at any time apparent) results in no deterioration in propulsive efficiency which remains high.

Owing to the limitation of linear assumptions, the non-planar and nonlinear features of waving plate and vortical sheets which may affect the flow and performance of waving plates significantly are not considered here. These remain to be improved and may be studied by a direct extension of the present method.

The suggestions and discussions on this paper given by referees are much appreciated.

REFERENCES

AHMADI, A. R. & WIDNALL, S. E. 1986 *J. Fluid Mech.* **162**, 261–282.

BLAKE, R. W. 1983 In *Fish Biomechanics* (ed. P. W. Webb & D. Weihs), pp. 177–213.

BLAKE, R. W. 1983 *Fish Locomotion*. Cambridge University Press.

CHENG, H. K. 1978 *University of Southern California, Dept. Aerospace Engng Rep. USCAE* 133.

CHENG, H. K. & MURILLO, L. E. 1984 *J. Fluid Mech.* **143**, 327–350.

CHENG, J. Y., ZHUANG, L. X. & TONG, B. G. 1989 *J. Hydrodyn.* **4**, 89–102.

CHOPRA, M. G. 1974 *J. Fluid Mech.* **64**, 375–391.

CHOPRA, M. G. & KAMBE, T. 1977 *J. Fluid Mech.* **79**, 49–60.

KANDIL, O. A., CHU, L. C. & TUREAND, T. 1982 *AIAA Paper* 82-0351.

KARPOUZIAN, G., SPEDDING, G. & CHENG, H. K. 1990 *J. Fluid Mech.* **210**, 329–351.

LAN, C. E. 1979 *J. Fluid Mech.* **93**, 747–765.

LIGHTHILL, M. J. 1975 *Mathematical Biofluiddynamics*. Philadelphia: SIAM.

WU, T. Y. 1961 *J. Fluid Mech.* **10**, 321–344.

WU, T. Y. 1971 *J. Fluid Mech.* **46**, Parts 1–3, 337–355, 521–568.

ZHUANG, L. X., SHIDA, Y. & TAKAMI, H. 1990 *Fluid Dyn. Res.* **5**, 321–336.